Appl. Phys. B 69, 429–433 (1999) / Digital Object Identifier (DOI) 10.1007/s003409900160

Applied Physics B
Lasers
and Optics

Multiple-pattern stability in a photorefractive feedback system

M. Schwab[1], **C. Denz**[1], **M. Saffman**[2]

[1] Institute of Applied Physics, Darmstadt University of Technology, Hochschulstr. 6, 64289 Darmstadt, Germany
(Fax: +49-6151/16-4123, Email: Michael.Schwab@physik.tu-darmstadt.de)
[2] Optics and Fluid Dynamics Department, Risø National Laboratory, Postbox 49, 4000 Roskilde, Denmark

Received: 22 June 1999/Revised version: 30 August 1999/Published online: 3 November 1999

Abstract. We report on the observation of a multiple-pattern stability region in a photorefractive single-feedback system. Whereas hexagonal patterns are predominant for feedback with positive diffraction length we show that a variety of stable non-hexagonal patterns are generated for certain negative diffraction lengths. For the same values of the control parameters square, rectangular, or squeezed hexagonal patterns are found alternating in time. Besides these pure states, we found a number of different mixed-pattern states. We review the linear stability analysis for this system and show that the special shape of the threshold curves in the investigated parameter region gives a first explanation for the occurrence of a multiple-pattern region.

PACS: 42.65.Sf; 42.65.Hw; 47.54.+r

The spontaneous formation of periodic spatial patterns is well known for a variety of nonlinear optical materials, for example atomic vapours [1], liquid crystals (Kerr slices) [2, 3], organic films [4], or photorefractives [5], where squares and squeezed hexagons were first observed in experiment [6]. Photorefractive materials are well suited for pattern observation since their intrinsically slow dynamics offers the opportunity to perform real-time measurements and observations. Moreover, low cw powers in the range of milliwatts are required and in the case of a diffusion-dominated crystal such as $KNbO_3$, no external voltage has to be supplied providing an all-optical pattern formation system. In all these systems, a single-feedback configuration creating two counterpropagating beams in the nonlinear optical medium gives rise to transverse modulational instabilities above a certain threshold. These instabilities generally lead to the formation of hexagonal patterns, which were first reported for a photorefractive system by Honda [5]. Following this pioneering work, various other publications offered improved insight into the stages of pattern formation in these photorefractive materials [7, 8]. A first approach to a nonlinear stability analysis [9] and studies of pattern dynamics due to angular misalignment and competition behaviour were published recently [10–12].

Our focus of interest is to investigate more complex patterns that may arise in the same configuration for a certain range of the diffraction length without changing the basic interaction geometry. Although some of these patterns were observed previously [6], the appropriate region of instability has not yet been investigated. Besides pure pattern states, such as squares, rectangles, or squeezed hexagons, we could observe a large number of different mixed states where two or more patterns coexisted. This variety of patterns leads to the question of manipulation, stabilization and control of these different pattern states which is currently of high interest [13–16]. The aim is to get defined access to different patterns, an essential condition to make use of spontaneous pattern formation in the growing field of optical information processing [17]. To make use of the different control schemes, it is absolutely necessary to gain knowledge about the different stability (and instability) regions of the present system. Thus, our aim in this paper is to get improved insight into the stages of pattern formation in this system and the parameter regions for different pattern types. A review of the linear stability analysis is given together with new results from this analysis. We combine these results with the occurrence of multiple patterns, thus giving an explanation for our experimental observations.

1 Linear stability analysis

The basic interaction geometry is depicted in Fig. 1. A plane wave of complex amplitude F is incident on a thick photorefractive medium with length l. The backward beam B is produced by reflection at a mirror at a certain position L behind the medium. Our analysis is not restricted to positive diffraction lengths since the $4f-4f$ configuration enables us experimentally to produce negative diffraction lengths which are essential for observing multiple-pattern stability. The principle function of the diffraction length L is to introduce a phase lag of the generated sidebands relative to the central beam. A diffusion-dominated medium such as $KNbO_3$ offers beam-coupling properties which are essential for pattern formation in this configuration. In this

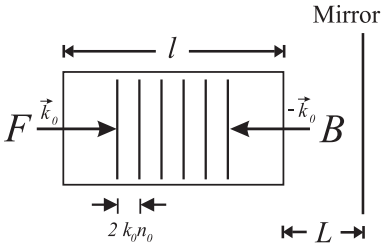

Fig. 1. Basic interaction geometry

case, a dynamic photorefractive grating with a grating vector of $2k_0n_0$ is written, with k_0 representing the wave number of the incident wave and n_0 the linear refractive index of the crystal.

The linear stability analysis presented here is based on the treatment by Honda and Banerjee given in [8]. It is derived from the standard photorefractive two-wave-mixing equations (known as Kukhtarev's equations [18]) and based on the assumption that reflection gratings are dominant in this configuration, which has been shown to be unstable against periodic perturbations. The usual equations for contradirectional two-beam coupling in a diffusion-dominated medium can be written in steady state as [8]

$$\frac{\partial F}{\partial z} - \frac{\mathrm{i}}{2k_0n_0}\nabla_\perp^2 F = \mathrm{i}\gamma\frac{|B|^2}{|F|^2+|B|^2}F\,,$$
$$\frac{\partial B}{\partial z} + \frac{\mathrm{i}}{2k_0n_0}\nabla_\perp^2 B = -\mathrm{i}\gamma^*\frac{|F|^2}{|F|^2+|B|^2}B\,. \qquad (1)$$

z is the direction of propagation, $\nabla_\perp = \frac{\partial^2}{\partial x^2} + \frac{\partial^2}{\partial y^2}$ denotes the transverse Laplacian, and $\gamma = \frac{\pi n_1}{\lambda}\exp(-\mathrm{i}\phi)$ is the complex photorefractive coupling constant, representing a measure for amplitude and phase transfer in the photorefractive two-wave-mixing process [18]. Here, λ is the wavelength of the incident waves, n_1 is a dimensionless factor measuring the modulation depth of the refractive index grating, and ϕ represents the relative phase shift of the refractive index grating with respect to the interference grating written by the beams. For the $KNbO_3$:Fe crystal we used in our experiments, this shift is known to be $\phi = \pi/2$ [19] yielding a purely imaginary coupling constant γ in the notation we use here. This in turn is known to cause pure energy-coupling between the two beams, i.e. energy is transferred from one beam to the other [19]. Performing a linear stability analysis for the system of partial differential equations (1) by applying weak spatial perturbations in the transverse plane and including the boundary conditions (representing the phase lag by feedback), one can obtain a threshold condition for modulational instability (see [8] for details):

$$\cos(wl)\cos(k_d l) + \frac{\gamma}{2w}\sin(wl)\cos(k_d(l+2n_0L)) + \frac{k_d}{w}\sin(wl)\sin(k_d l) = 0\,, \qquad (2)$$

with $w = \sqrt{k_d^2 - \gamma^2/4}$ and $k_d = \frac{k_\perp^2}{2k_0n_0}$, where $k_\perp$ represents the transverse wavevector $k_\perp^2 = k_x^2 + k_y^2$ and thus the sideband angle $\theta = k_\perp/k_0$ in experiment. L is the (virtual) mirror distance from the medium and l denotes the length of the crystal. The threshold condition therefore reads in a more simplified form as $f(\theta, \gamma, L) = 0$, representing a purely real threshold condition for all parameter values. Given a certain mirror position L, a threshold curve $f(\theta, \gamma) = 0$ can be derived, where the absolute minimum provides information about the unstable sideband angle θ at a certain mirror position (see Fig. 2). If the relative minima of this threshold curve are numbered consecutively, the values of the threshold coupling strength depending on the mirror position for the first to fourth instability "balloon" can be plotted leading to Fig. 3a. The characteristic shape of the curve indicates that a certain coupling strength is necessary to observe patterns in the region around $n_0L/l = -0.5$. This corresponds to previously reported results that for a lower coupling strength, no pattern formation can be observed in this parameter region [10, 11]. Note also the characteristic dip at a value for the diffraction length of $n_0L/l = -0.5$ and the oscillations appearing for the higher order curves. The corresponding values for the sideband angle θ in the threshold condition lead to the curve displayed in Fig. 3b. One can see clearly the abnormal behaviour of the sideband angle-curve (Fig. 3b) in a region near $n_0L/l = -0.5$, where a nearly vertical rise of the curve appears. This typical shape of the curve also appears in the higher order curves and is therefore a special property of this nonlinear feedback system. It may also be a generic feature of negative diffraction lengths in cubic material, but this investigation is not in the scope of this paper. However, the special shape of the curves in Fig. 3a,b may give rise to unexpected patterns in this parameter region. Figure 3a,b extends previous results of the linear stability analysis [8, 9], taking into account negative diffraction lengths and higher order instability balloons. However, a nonlinear stability analysis is still required for explaining the occurrence of different pattern types. The reason for the occurrence of these patterns can only be found by a nonlinear analysis, since a linear stability analysis only accounts for the occurrence of a special transverse wavevector to become unstable when excited beyond the instability threshold. The stability of hexagons for small positive values of L was shown recently [9], an appropriate analysis for negative diffraction lengths is still not available and not within the scope of this paper. We will concentrate on experimental investigations in this parameter region of small negative diffraction lengths.

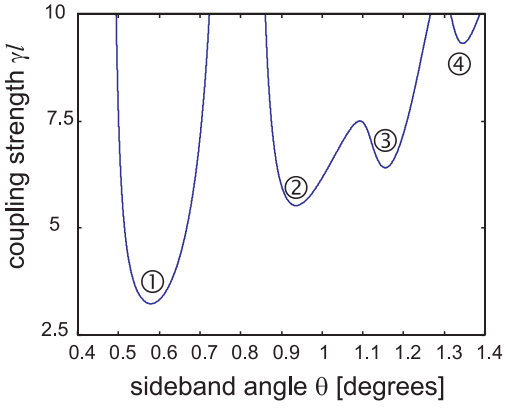

Fig. 2. Example of a threshold curve for $n_0L/l = 0.6$

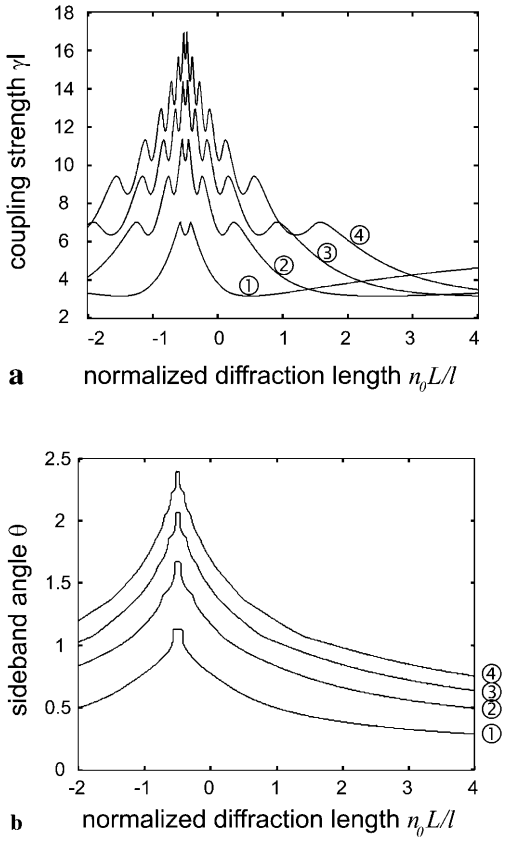

Fig. 3a,b. Results from the linear stability analysis. **a** Minimal coupling strength for different normalized mirror positions n_0L/l. **b** Theoretical values for the minima of the threshold curves for varying values of L

2 Multiple-pattern stability

The experimental setup is depicted in Fig. 4. Light obtained from a frequency-doubled cw Nd:YAG laser operating at $\lambda = 532\,\text{nm}$ with a coherence length of some metres is focused by lens L1 of focal length $f = 600\,\text{mm}$ onto the exit face of an iron-doped $KNbO_3$ crystal ($l = 5\,\text{mm}$), producing a spot with a Gaussian diameter of 320 μm. The crystal was slightly inclined (about 4°) in order to avoid undesired back-reflections from the crystal surfaces. By means of a $4f - 2L - 4f$-system with $f = 100\,\text{mm}$, the incoming beam is back reflected, thus providing the counterpropagating beam. Considering ABCD-matrix formalism, this configuration can be shown to be completely equivalent to a simple single-mirror feedback configuration. Thus, a virtual mirror with a distance of L from the photorefractive medium is obtained. The basic advantage of this system is that negative diffraction lengths can be achieved, which allow one to access a broader range of stationary patterns, including squares and rectangles. The laser beam is linearly polarized along the crystal a-axis to exploit the large r_{13} component of the electrooptic tensor in this direction, resulting in a minimum input power for pattern observation of just 0.5 mW. A beam splitter between the focusing lens and the photorefractive medium enables one to observe the far field, and by means of a lens and a microscope system, the near field, respectively. The direction of the crystal c-axis is arranged to give rise to depletion of the incoming and amplification of the backward reflected beam, a configuration that is necessary for the observation of transverse structures in this material. The reflectivity of the feedback system including all elements was measured to be $R = 83\%$.

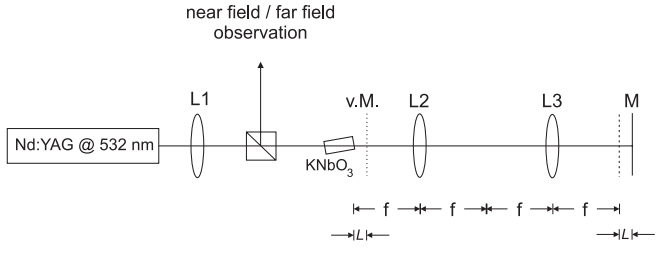

Fig. 4. Experimental setup. M = mirror, v.m. = virtual mirror, L = diffraction length

For positive diffraction lengths stable hexagonal patterns are always seen, as depicted in Fig. 5a. Higher order harmonics of the hexagonal pattern are clearly apparent in experiment. They saturate the explosive instability of the first-order hexagon and are essential for the stability of a hexagonal pattern [9]. This hexagonal structure is well known to be dominant for many different nonlinear optical materials and is reported for a number of other non-optical pattern-forming systems. However, when the virtual mirror is shifted into the crystal, i.e. when negative diffraction lengths are achieved, a remarkable pattern transition occurs: in a small parameter region of the diffraction length around $n_0L/l = -0.5$, different non-hexagonal structures may appear. Square patterns, squeezed hexagonal, rectangular, or parallelogram-shaped structures (see Fig. 5b–e) can be realized as stable pure solutions. The patterns were stable for a long period of time ($t \gg 1000\tau$), where τ denotes the time constant for this system, in this case defined as the mean build-up time of a pattern which was in the range of 0.5–1 s in the experiments reported here, depending on the input intensity. Temporal alternation of different patterns due to disturbances in the system was also possible on much larger timescales ($t \geq 20\,\text{s}$) than the usual build-up time of a pattern. Besides these pure stable states, also mixed states can be observed, where different patterns coexist on the same or different transverse scales. Even here, this coexistence could be realized to be stable in space for times much longer than the characteristic time constant of the system. Selected mixed-pattern states are displayed in Fig. 6a–d. One can see the rich variety of possible patterns regarding their transverse $\boldsymbol{k}$-vectors and orientation in space. The condition for the occurrence of a special pure- or mixed-pattern type in the multiple-pattern region is still unclear. For this reason, we call this parameter region *multiple-pattern region* since a clear parameter-dependent behaviour

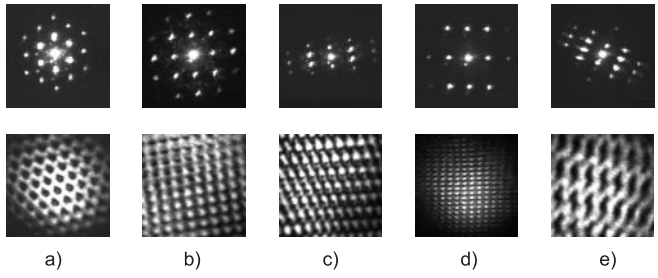

Fig. 5a–e. Experimentally obtained pure pattern states. **a** Predominant hexagonal structure. **b–e** Other pattern geometries for the multiple-pattern region $n_0 \approx -0.5$. The intensity incident on the crystal was $I = 2.4\,\text{W/cm}^2$

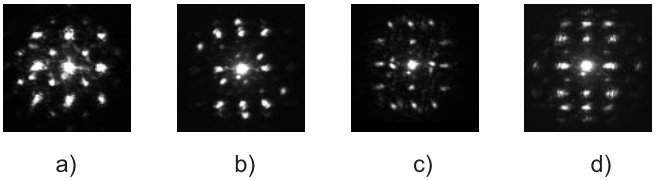

Fig. 6a–d. Examples for the occurrence of mixed states: two square patterns with different scales and orientation (**a**), two rectangles with same scale and different orientation (**b**), two rectangles and square pattern (**c**), square pattern and rectangle (**d**). All pictures taken for an intensity of $I = 2.4\,\mathrm{W/cm^2}$ and mirror positions in the multiple-pattern region

of the different pattern types was not obtained. A rich variety of patterns was accessible, as well as a large set of transverse ***k***-vectors as shown in Figs. 5 and 6, even for the same diffraction length. Outside this multiple-pattern region, no patterns other than hexagonal ones can be observed experimentally.

Previously [10, 11], we reported a remarkable pattern collapse for the region of negative diffraction length where we now observe multiple-patterns. The pattern collapse, or absence of patterns, was explained as a result of the photorefractive coupling strength being too low for the observation of transverse structures. In the experiments reported here a different crystal was used with about twice as large nonlinearity ($\gamma l \approx 4$) which accentuates the necessity of sufficient nonlinearity for observing non-hexagonal patterns in the regime of negative diffraction length. The value of the coupling strength given here is a raw experimental value that was deduced from measurements of small signal gain, and does not take into account high modulation-depth effects that are present when counterpropagating beams of comparable intensity write a reflection grating. This may account for the discrepancy between the measured nonlinearity and the theoretical threshold values in Fig. 3 required for pattern formation in the multiple-pattern region. This point is currently under investigation.

Though a nonlinear stability analysis has not been performed for negative diffraction lengths, detailed investigations of the results of the linear stability analysis taking into account higher order instability balloons may already give useful information about the pattern type. Figure 7 shows the measured values for the hexagon instability angle θ as a function of the normalized diffraction length $n_0 L/l$ (virtual mirror

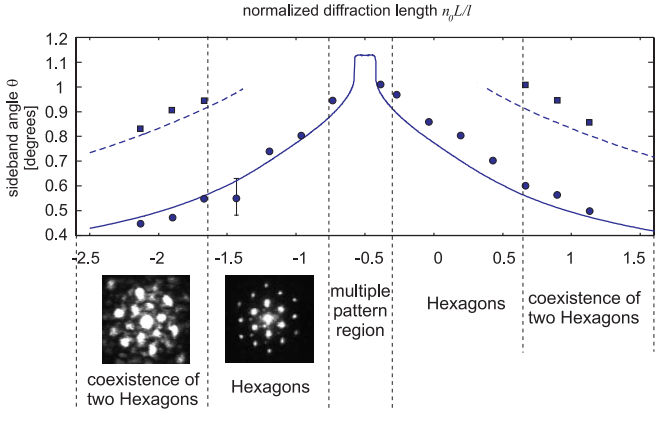

Fig. 7. Sideband angle θ as function of the normalized diffraction length $n_0 L/l$ for an incident intensity of $I = 2.4\,\mathrm{W/cm^2}$. The theoretical curve is displayed together with experimental values for the transverse scale (*circles* and *squares*)

is inside the crystal for values $-1 \le n_0 L/l \le 0$) together with the theoretical results of the linear stability analysis (first and second instability balloon). The measured values agree well with the theoretical curves. As predicted in [10], a coexistence of two transverse ***k***-vectors appears for larger positive or negative diffraction length as indicated in the figure. Here, a second instability balloon (see Fig. 3 in [10]) takes the absolute minimum of the instability curve thus leading to a degeneration of the transverse wave-vector. This leads to a coexistence of two hexagons on two transverse scales tilted by 30° relative to each other. The multiple-pattern region described earlier is also indicated in the figure. A large number of various transverse ***k***-vectors occur for $-0.7 \le n_0 L/l \le -0.3$, being too numerous to be displayed in Fig. 7. One can see clearly that for parameter values $n_0 L/l = -0.57$ and $n_0 L/l = -0.43$ the curve in Fig. 7 shows a nearly vertical rise indicating that a whole band of transverse ***k***-vectors will participate in the stage of pattern formation, thus explaining the variety of transverse ***k***-vectors. However, this explanation does not hold for $n_0 L/l = -0.5$ (flat region of this curve) where sideband angles up to 2.7° could be observed for the case of rectangular patterns. This problem is still under investigation.

3 Discussion and conclusion

We have analyzed a parameter region where a photorefractive feedback system produces a variety of different spatial patterns. With our experimental configuration, we are able to access a broader parameter region including negative diffraction lengths, which allow the observation of squares, squeezed hexagonal, or rectangular patterns. The occurrence of non-hexagonal patterns is restricted to a small parameter region where the virtual mirror is placed inside the crystal. This *multiple-pattern region* coincides with an unusual shape of the corresponding curves for pattern size vs. diffraction length derived from a linear stability analysis. In the multiple-pattern region, a temporal alternation of different patterns is possible. This is, to the best of our knowledge, the first observation of a multiple-pattern parameter region. This observation may not be restricted to photorefractives and could be observed in other optical-pattern-forming systems.

We also discovered a coexistence of two hexagonal patterns which can be explained by the existence of two instability balloons competing for the absolute minimum of the threshold curve. We could clearly separate the parameter regions for coexisting hexagons, pure hexagons, and multiple stability.

Acknowledgements. We would like to acknowledge helpful support by Prof. Dr. T. Tschudi. M. Schwab acknowledges partial support by a FAZIT scholarship and the Danish Research Academy. The research of M. Saffman was supported by the Danish Natural Science Research Council.

References

1. G. Grynberg, E. LeBihan, P. Verkerk, P. Simoneau, J.R.R. Leite, D. Bloch, S. Le Boiteux, M. Ducloy: Opt. Commun. **67**, 363 (1988); J. Pender, L. Hesselink: J. Opt. Soc. Am. B **7**, 1361 (1990)
2. R. Macdonald, H.J. Eichler: Opt. Commun. **89**, 289 (1992); B. Thüring, R. Neubecker, T. Tschudi: Opt. Commun. **102**, 111 (1993)
3. M.A. Vorontsov, A.Yu. Karpov: Opt. Lett. **20**, 2466 (1995); M.A. Vorontsov, A.Yu. Karpov: J. Opt. Soc. Am. B **14**, 34 (1997)

4. J. Glückstad, M. Saffman: Opt. Lett. **20**, 551 (1995)
5. T. Honda: Opt. Lett. **18**, 598 (1993)
6. T. Honda, H. Matsumoto, M. Sedlatschek, C. Denz, T. Tschudi: Opt. Commun. **133**, 293 (1997)
7. M. Saffman, A.A. Zozulya, D.Z. Anderson: J. Opt. Soc. Am. B **11**, 1409 (1994); T. Honda, H. Matsumoto: J. Opt. Soc. Am. B **11**, 1983 (1994); T. Honda: Opt. Lett. **20**, 851 (1995)
8. T. Honda, P.P. Banerjee: Opt. Lett. **21**, 779 (1996)
9. P.M. Lushnikov: Zh. Éksp. Teor. Fiz. **113**, 1122 (1998) [JETP **86**, 614 (1998)]
10. C. Denz, M. Schwab, M. Sedlatschek, T. Tschudi, T. Honda: J. Opt. Soc. Am. B **15**, 2057 (1998)
11. M. Schwab, M. Sedlatschek, B. Thüring, C. Denz, T. Tschudi: Chaos, Solitons Fractals **10**, 701 (1999)
12. A.V. Mamaev, M. Saffman: Opt. Lett. **22**, 283 (1997)
13. W. Lu, D. Yu, R.G. Harrison: Phys. Rev. Lett. **76**, 3316 (1996); R. Martin, A.J. Kent, G. D'Allesandro, G.L. Oppo: Opt. Commun. **127**, 161 (1996)
14. R. Martin, A.J. Scroggie, G.-L. Oppo, W.J. Firth: Phys. Rev. Lett. **77**, 4007 (1996)
15. A.V. Mamaev, M. Saffman: Phys. Rev. Lett. **80**, 3499 (1998)
16. S. Juul Jensen, M. Schwab, C. Denz: Phys. Rev. Lett. **81**, 1614 (1998)
17. M.A. Vorontsov, W.B. Miller (Eds.):*Self-Organization in Optical Systems and Applications in Information Technology* (Springer, Berlin, Heidelberg 1995)
18. N.V. Kukhtarev, V.B. Markov, S.G. Odulov, M.S. Soskin, V.L. Vinetskii: Ferroelectrics **22**, 961 (1979)
19. L. Solymar, D.J. Webb, A. Grunnet-Jepsen: *The Physics and Applications of Photorefractive Materials* (Clarendon Press, Oxford 1996)